어안렌즈사용 CCTV이미지에서 차량 정보 수집의 성능개선을 위한 디블러링 알고리즘

정회원 이 인 정*

De-blurring Algorithm for Performance Improvement of Searching a Moving Vehicle on Fisheye CCTV Image

In-Jung Lee* *Regular Member*

요 약

CCTV이미지에서 교통정보를 수집하려고 할 때 관측자가 카메라를 움직이면 설치된 검지영역이 손실되고 복원하려고 해도 기계적 오차로인해 어려움을 겪게 된다. 그래서 어안이나 거울을 이용하면 카메라를 움직이지 않아도 된다. 하지만 이러한 상황하에서 가장 큰 문제점은 영상의 왜곡이다. 본 논문에서는 이러한 왜곡을 극복하기 위해 비선형 확산 방정식을 이용한 분할과 이 영역에디포메이션을 적용하여 디블러링 한 후 차량정보 수집을 시도한 결과 이전 결과보다 5% 향상된 결과를 얻었다.

Key Words : De-Blurring, Deformation, Fisheye Image, Nonlinear Diffusion Equation

ABSTRACT

When we are collecting traffic information on CCTV images, we have to install the detect zone in the image area during pan-tilt system is on duty. An automation of detect zone with pan-tilt system is not easy because of machine error. So the fisheye lens attached camera or convex mirror camera is needed for getting wide area images. In this situation some troubles are happened, that is a decreased system speed or image distortion. This distortion is caused by occlusion of angled ray as like trembled snapshot in digital camera. In this paper, we propose two methods of de-blurring to overcome distortion, the one is image segmentation by nonlinear diffusion equation and the other is deformation for some segmented area. As the results of doing de-blurring methods, the de-blurring image has 15 decibel increased PSNR and the detection rate of collecting traffic information is more than 5% increasing than in distorted images.

Ⅰ. Introduction

Closed Circuit Television(CCTV) systems have been extensively deployed to monitor freeways in urban areas. While CCTVs have proven to be very effective in monitoring traffic flows and supporting incident management, they simply provide images that must be interpreted by trained operators[1]. These large and expensive video systems have, however, limited functionality. Recently, the university or scientific transportation institution have been researching to extend the CCTV functionality for the most part of detection system via CCTV images, for example integrating CCTV sur-

※ 본 연구는 2009년도 호서대학교의 재원으로 학술연구비 지원을 받아 수행된 연구임(2009-0231)
* 호서대학교 교양학부(leeij@hoseo.edu)
논문번호 : KICS2009-06-252, 접수일자 : 2009년 6월 19일, 최종논문접수일자 : 2010년 3월 3일

veillance with video image vehicle detection system(VIVDS)[1]-[3] and detection weather or road surface condition using CCTV[4]. Almost all of CCTV surveillance system must have a pan, tile and zoom(PTZ) drive by reason that CCTV system cannot be displayed bidirectional or more wide area of traffic flow simultaneously. If operators want to view the 360 degree all round area extremely at the same time, four CCTV cameras or convex-mirror [18] or fisheye lens are needed. And if an operator has a single camera when PTZ is on, the detect zone has to install in the CCTV images, this installing system is not easy because of machine error. When we use an improved CCTV added fisheye lens or convex mirror which has a more widely view than ordinary CCTV system, fisheye view is not a familiar image in human eye, distortion across the hemispherical field of view shown as Fig.1.

Then operators in Traffic Management Center (TMC) cannot be monitoring the traffic situation via naked CCTV image with fisheye. But, as in [17], traffic information can be collected within convex image. So the tracking of moving object can be detected, but the speed of vehicle is not properly adaptive in this situation. Also we have to need a transformation algorithm fisheye view into de-warped image.

And when fisheye image spread out in transformation of fisheye view into de-warped image, the blurring occurred because small size image of fisheye view is spread out to larger size of de-warped image shown as Fig.2.

Let a point p(x,y,z) be in the fisheye image and a corresponding point q(a,b) be in flat image as Fig.3. Then we can transform p(x,y,z) to q(a,b)

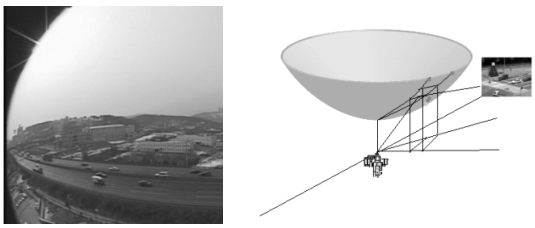

Fig.1. fisheye view or convex mirror view

Fig.2. The blurring is occurred because small size image of fisheye view is spread out to larger size of de-warped image

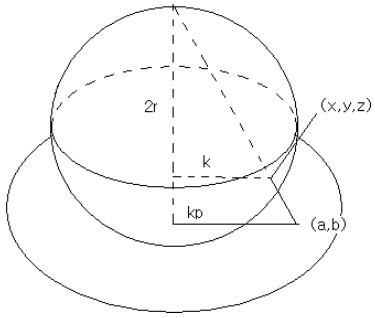

Fig.3. A matching from one point (x,y,z) on a sphere to the point (a,b) on disc

through the equation 1,2, where r is a radius of fish-eye image. So the de-warped image is shown by this transform in Fig.4.

$$a = \frac{2xr}{2r-z} \qquad \text{Eq1.}$$

$$b = \frac{2yr}{2r-z} \qquad \text{Eq2.}$$

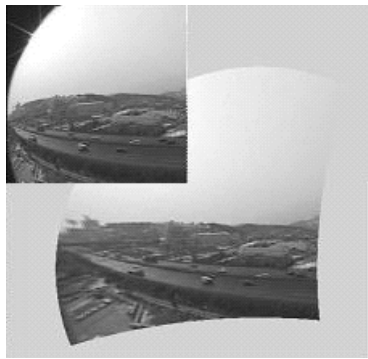

Fig.4. A transformed image from a fish-eye image applying equation 1,2

In the paper [14], the de-blurring transformation algorithm with nonlinear equation and shift expansion method such that the de-warped image have to be restored according to expansion of DOV and backward solution[9]-[13] of wave equation by the reflection and interferenceof light. But, this method has large number of calculation. In this paper, we propose nonlinear diffusion equation and deformation methodin section II. Also we shall show performance of moving vehicle detection performed with de-blurring image in section III.

Ⅱ. Nonlinear Diffusion Equation and Deformation

In this section, we introduce a discontinuous force function, resulting in a system as equation 3, that has discontinuous right-hand side(RHS)[15].

$$\frac{\partial u_n}{\partial t} = \frac{1}{m_n}(F(u_{n+1} - u_n) - F(u_n - u_{n-1})),\ n = 1,2,3,\dots N \quad \text{Eq3.}$$

where u_n is a discretized signal and F is a force function.

Such equations received much attention in control theory because of the wide usage of relay switches in automatic control systems. More recently, deliberate introduction of discontinuities has been used in control applications to drive the state vector onto lower-dimensional surfaces in the state space. As we will see, this objective of driving a trajectory onto a lower-dimensional surface also has value in image analysis and in particular in image segmentation. Segmenting a signal or image, represented as a high-dimensional vector, consists of evolving it sothat it is driven onto a comparatively low-dimensional subspace which corresponds to a segmentation of the signal or image domain into a small number of regions. The type of force function of interest to us here is illustrated in Fig.6.

More precisely, we wish to consider force functions which satisfy the following properties equation 4 such as

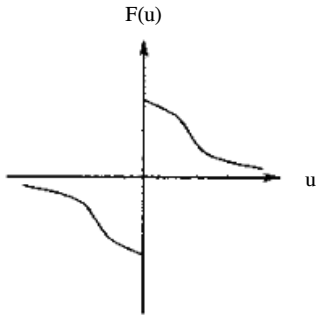

Fig.6. Force function for a stabilized inverse diffusion equation

$$F'(v) \le 0 \text{ for } v \neq 0,$$
$$F(0^+) > 0$$
$$F(v_1) = F(v_2) \text{ if and only if } v_1 = v_2 \quad \text{Eq4.}$$

However, because of the discontinuity at the origin of the force function in Fig.6, there is a question of how one defines solutions of equation 4 for such a force function. Indeed, if equation 4 evolves toward a point of discontinuity of its RHS, the value of the RHS of equation 4 apparently depends on the direction from which this point is approached, making further evolution non-unique. We therefore need a special definition of how the trajectory of our evolution proceeds at these discontinuity points. For this definition to be useful, the resulting evolution must satisfy well-posed properties, that is the existence and uniqueness of solutions, as well as stability of solutions with respect to the initial data. Viewed as a segmentation algorithm, our evolution can be summarized as follows.

1) Start with the trivial initial segmentation: each sample is a distinct region.
2) Evolve equation 5 until the values in two or more neighboring regions become equal. $\frac{\partial u_{n_i}}{\partial t} = \frac{1}{m_{n_i}}(F(u_{n_{i+1}} - u_{n_i}) - F(u_{n_i} - u_{n_{i-1}}))$

$$u_{n_i} = u_{n_i+1} = \cdots = u_{n_i+m_{n_i}-1} \quad \text{Eq5.}$$

where

$$i = 1,2,3,\dots p,\ 1 = n_1 < n_2 \dots < n_{p-1} < n_p \le N,$$
$$n_{i+1} = n_i + m_{n_i}$$

3) Merge the neighboring regions whose values are equal.
4) Go to step 2.

Applying this algorithm to a 256*256 gray image, we obtain a result image as follows Fig.7.

Nevertheless, we can not find segmented face area which is vary important region for de-blurring. Under the same stability of Eq.5, we propose a parameter α such as

$$\frac{\partial u_{n_i}}{\partial t} = \frac{1}{m_{n_i}}\left(F\left(u_{n_{i+1}} - u_{n_i}\right) - \alpha F\left(u_{n_i} - u_{n_{i-1}}\right)\right)$$
$$u_{n_i} = u_{n_i+1} = \cdots = u_{n_i+m_{n_i}-1} \qquad \text{Eq6.}$$

where

$$i = 1,2,3,\dots p,\ 1 = n_1 < n_2 \dots < n_{p-1} < n_p \le N,$$
$$n_{i+1} = n_i + m_{n_i}$$

Applying this Eq6. to a 256*256 gray image, we obtain a result image as follows Fig.8.

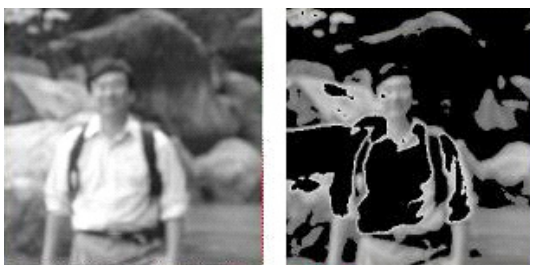

Fig.7. A result image is right image by applying segmentation algorithm to left image

Fig.8. A result image applied by Eq6

In this segmented area, the deformation method is used to get de-blurring image[16]. The deformation equation is defined by equation 7, let a surface be Ω,

$$\frac{\partial \Omega}{\partial t} = \alpha(s,t)\mathrm{T} + \beta(s,t)\mathrm{N}\ \ \Omega(s,0) = \Omega_0(s) \qquad \text{Eq7.}$$

where T is a tangent and N is a normal vector, α and β are arbitrary function. From this equation 7, we define a curvature deformation equation. Let a function of surface be $z = \varphi(x,y,t)$,

$$\frac{\partial \Omega}{\partial t} = -K\mathrm{N}$$
$$\Omega(s,0) = \Omega_0(s) \qquad \text{Eq8.}$$
where $K = \frac{(\varphi_{xx}\varphi_y^2 - 2\varphi_{xy}\varphi_x\varphi_y + \varphi_{yy}\varphi_x^2)}{(\varphi_x^2+\varphi_y^2)^{\frac{2}{3}}}$.

Applying equation 8 at a segmented area, we obtain a de-blurring image as Fig.9.

So we apply the CCTV image, we have a de-blurred image as in Fig.10. For evaluation of de-blurring effectiveness, we can choose one line of image in Fig.11, and compute the cross section in Peek Signal To Noise Rate(PSNR), Equation 9, of this data.

Fig.9. A de-blurring image is obtained at right from blurring image at left

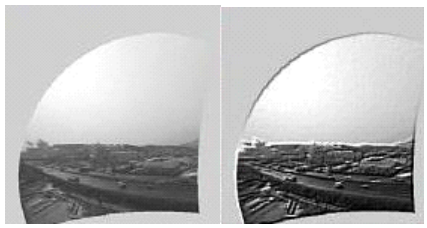

Fig.10. Blurred image and their de-blurring image

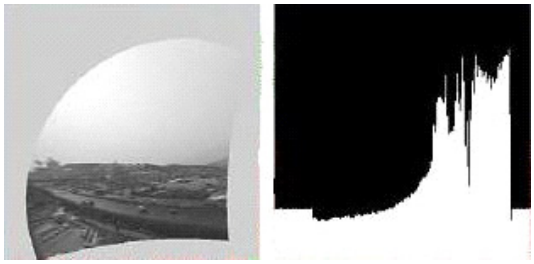

(a) The cross section of blurring image of one line

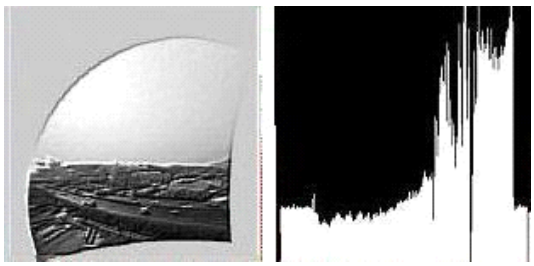

(b) The cross section of de-blurring image with diffusion equation and deformation

Fig.11. The cross section of blurring image of one line (a) and the de-blurring image with diffusion equation and deformation

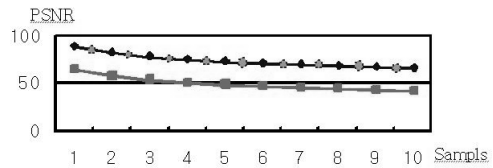

Fig.12. The circle line is PSNR with de-blurred image and rectangle line is without de-blurring

$$PSNR = 20\log_{10}^{(\frac{255}{\sigma})} \qquad \text{Eq9.}$$

Where, σ is mean squared errors. The Fig.12 shows the difference of PSNR about 20 decibels with or without de-blurring.

Ⅲ. Performance of Moving Vehicle Detection

We transform a fish-eye image to flat image in order to collecting traffic information and then we install the detection zone on the transformed flat image as in Fig.13.

But, because of image distortion arising transform process, some trouble has happened for finding a vehicle speed or calculating vehicle numbers amount per properly chosen times as about 3 seconds. So as section II, de-blurring is applied to flat image in order to performance of recognition. Actually, the tracking vehicle is doing as in Fig.14 by using difference image and its binary image. In order to get some information from the binary difference image, we decide the area rectangle of moving vehicle as the Fig.15. And we use the equation 10 as for a set R of one line-segment along ① or ②, a binary function $\text{OccFlaggs} : R \rightarrow \{0,1\}$ by

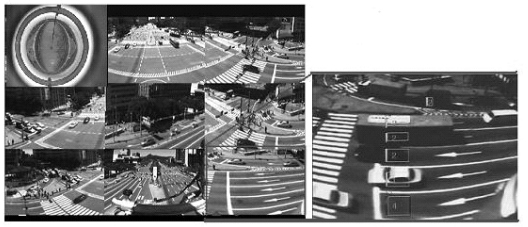

Fig.13. The detection zone of collecting traffic information in a flat image

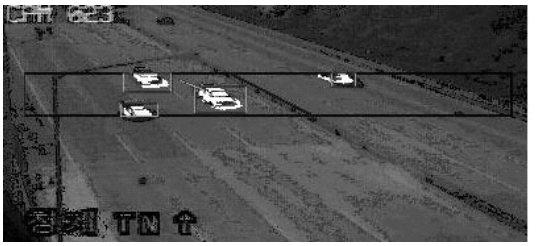

Fig.14. The detection zone for tracking vehicle

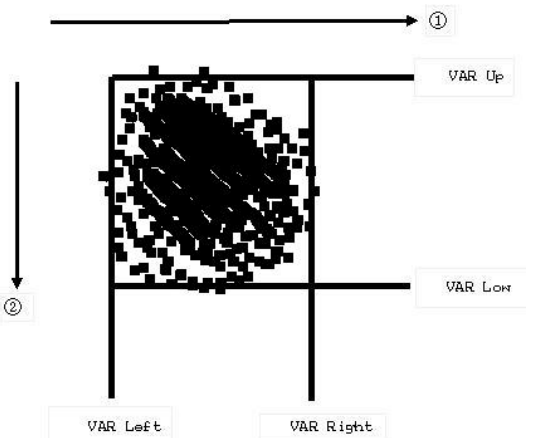

Fig.15. The area rectangle of moving vehicle

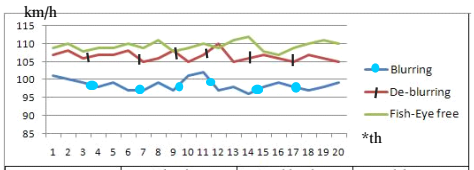

	Blurring	De-blurring	Fish-eye
mean	98.5	106.6	109.5
stdev	1.573	1.317	1.234

Fig.16. The vehicle speed of blurring, de-blurring and fish-eye free camera image 20th experiments from the same video file

$$OccFlags(x) = \begin{cases} 1 & \text{if } x > \lambda \\ 0 & \text{othewise} \end{cases} \quad \text{Eq10.}$$

Where $x = \frac{1}{N}\sum_{i}^{N-1} p_{i,j}$ along ② and $x = \frac{1}{N}\sum_{j}^{N-1} p_{i,j}$ along ① $p_{i,j}$ is 0 or 1 that is a value of binary pixel and λ is a deciding factor. The factor λ is obtained by experimental data which is about 20%. But, in this situation we miss the correct line and misread for blurred image, hence get more wide area than real area. Because of this reason, the traffic information is not correct. In Fig. 16, we show some experimental results of vehicle speed compared blurring image arising flat transformation and de-blurring image and fish-eye free camera image. Those experimental processes are played 20th from the same saved video file images. We show that using de-blurring image has 5% increasing performance in aspect to detecting rate than using blurring image. In spite of de-blurring, the performance of flat transformed image is not better than fish-eye free camera image. In this experimental process, almost every speed data is in the interval 2-σ distance from the mean, it is evidence that this experimental system is stable.

Ⅳ. Conclusions

An automation of detect zone with pan-tilt system is not easy because of machine error. So the fish-eye lens attached camera or convex mirror camera is needed for getting wide area images. In this situation some troubles are happened, that is a decreased system speed or image distortion. This distortion is caused by occlusion of angled ray as like trembled snapshot in digital camera. In this paper, we propose two methods of de-blurring to overcome distortion, the one is image segmentation by nonlinear diffusion equation and the other is deformation for some segmented area. As the results of doing de-blurring methods, the de-blurring image has about 20 decibel increased PSNR in Fig.12 and the detection rate of collecting traffic information is more than 5% increasing than in distorted images.

References

〔1〕 S. Namkoong, H. Tanikella, B. Smith, “Design and Field Evaluation of a System Integrating CCTV Surveillance with Video Image Vehicle Detection Systems (VIVDS),” *Paper submitted for presentation at the 2005 Annual Meeting of the Transportation Research Board and publication in the Transportation Research Record,* 2004. 7.

〔2〕 Pack, M.L., “Automatic Camera Repositioning Techniques for Integrating CCTV Traffic Surveillance Systems With Video Image Vehicle Detection Systems,” *Masters Thesis in Engineering, University of Virginia, Charlottesville*, VA, 2002.

〔3〕 In J. Lee, Joon Y. Min, “Development of an Algorithm for Automatic Installation of Detection Area in CCTV Image on Highways,” *Proc. of the International Conference on Image Science, Systems and Technology*, Jun., 26-29, 2000, pp.381-386.

〔4〕 Kenichi W. et. al. “A Study on Sensing System for Running Road Surface Conditions in ITS,” *Proceedings of 10th World Congress on Intelligent Transport Systems*, Madrid, Spain, Nov., 2003.

〔5〕 Sang H. Jung, “A Study on the Graphic Compensation of Warping Image Induced to Wide Angle Lens,” *Masters Thesis in Industry and Engineering, Seoul National University of Technology*, 2003.

〔6〕 T.F. Chan, G.H. Golub, P. Mulet, “A Nonlinear

Primal-Dual Method for Total Variation-Based Image Restoration," *SIAM Journal on Scientific Computing*, Vol.20, No.6, 1999, p.1964.

〔7〕 T. F. Chan, C. K. Wong, "Total Variation Blind De-convolution," *IEEE Transactions on Image Processing*, Vol.7, No.3, 1998, p.370.

〔8〕 A. Marquina, S. Osher, "Explicit Algorithms for a New Time Dependent Model Based on Level Set Motion for Nonlinear Deblurring and Noise Removal," *UCLA CAM Report 99-5, Department of Mathematics, University of California*, Los Angeles, 1999.

〔9〕 N. Moayeri, K. Konstantinides, "An Algorithm for Blind Restoration of Blurred and Noisy Images," *Technical Report HPL-96-102, Hewlett-Packard*, 1996.

〔10〕 Dupont, T. L, "Estimates for Galerkin methods for second-order hyperbolic equations," *SIAM J.Numer.Anal.* 10, 392-410, 1973.

〔11〕 Claudio Canuto M.Yousuff Hussaini Alfio Quarteroni Thomas A. Zang, "Spectral Methods in Fluid Dynamics," *Springer_Verlag,* 1988.

〔12〕 Yves Truginy, "Product approximation for non-linear Klein Gordon equations," *IMA journal of Numerical Analysis*. 9, 449-462, 1990.

〔13〕 In-Jung Lee, "Numerical Solution for Nonlinear Klein-Gordon Equation by Using Lagrange Polynomial Interpolation with a Trick," *The KIPS Transactions Part A*, Vol.11-A No.7, 2004, pp.571-576.

〔14〕 In J. Lee, Seong J. Namkoong, Joon Y. Min, "Expanding Degree of View of CCTV Camera Video Image and De-blurring with Nonlinear Equation". *Proceedings of 10th World Congress on Intelligent Transport Systems* Oct., 9-12, 2007, pp.485-489.

〔15〕 I. pollak, A. S. Willsky, "Image Segmentation and Edge Enhancement with Stabilized Inverse Diffusion Equations." IEEE Transactions on Image Processing, Vol.9, No.2, 256-266, 2000.

〔16〕 B. B. Kimia, K. Siddiqi, "Geometric Heat Equation and Nonlinear Diffusion of Shapes and Images. Computer Vision and Image Understanding." Vol.64, No.3, pp.305-322, 1996.

〔17〕 K. Yamazawa, N. Yokoya, " Detecting Moving Objects from Omnidirectional Dynamic Images Based on Adaptive background Subtraction." ICIP2003, pp.210-215, 2003.

〔18〕 H. Huang, H. Hong, "Estimation of Omnidirectional Camera Model with One Parametric Projection," LNCIS 345, pp.827-833, 2006.

이 인 정 (In-Jung Lee) 정회원

1981년 전남대학교 수학과 이학사

1984년 중앙대학교 수학과 이학석사

1990년 중앙대학교 수학과 이학박사

2002년 아주대학교 전자공학과 공학박사

1992년~현재 호서대학교 교양학부 교수

<관심분야> 영상신호처리, 수치해석, 인공지능